Permeation grouting of an upstream tailing dam: a feasibility study

Katia Boschi
Geomechanics Group, CIMNE, Barcelona, Spain

Marcos Arroyo
CIMNE – Universitat Politècnica de Catalunya – BarcelonaTech, Barcelona, Spain

Daniel Alejandro Burbano
Department of Civil and Environmental Engineering, Universitat Politècnica de Catalunya, Barcelona, Spain

Giovanni Spagnoli
DMT GmbH & Co. KG., Germany

ABSTRACT: The presence of potentially liquefiable deposits in tailing dams represents a serious hazard, as is now increasingly clear that liquefaction triggering may occur in unanticipated ways. For legacy dams in which this hazard is already present, intervention alternatives are sought to mitigate the associated risks of liquefaction failure. One interesting possibility is to use targeted ground improvements of tailings within the structural zone of the dams, so that they become non-liquefiable. Liquefaction remediation technologies that are relatively gentle would be preferable, as the possibility of triggering liquefaction during the ground improvement operation itself cannot be lightly discarded. Permeation grouting is a classical soil improvement technology that has been renovated with the apparition of new permeating agents, such as colloidal silica suspensions (CS). Permeation grouting of CS consists in low-pressure injections leading to CS treated soils characterized by a significantly reduced liquefaction potential. CS grout has a complex rheology that is best described by a Bingham model whose parameters change in time. This paper presents design tools that incorporate this complexity and allow both a safer and more realistic design of permeation treatments. As an application example, we study a case based on the Merriespruit tailing dam, which failed by static liquefaction. It is concluded that CS permeation could realistically offer a potential solution to reduce instability risk of some tailing storage facilities (TSF).

1 INTRODUCTION

Many existing active and legacy tailing storage facilities (TSF) contain materials that are susceptible to liquefaction. The presence of such materials increases the risk of brittle failure modes and the impact or consequence of failures. The recent ICMM Good Practice Guide (International Council for Mining and Metals; ICMM, 2021) advises to avoid liquefiable materials on the structural zone of upstream TSF and to use lower bound strengths (i.e. liquefied undrained strength) in stability analyses involving those materials. If potentially liquefiable materials are already present in the structural zone, it is likely that the risks will be deemed unacceptable without some intervention. Most interventions for stability improvement take the form of section modification via buttressing, but there may be also circumstances in which alternative solutions to buttressing may be sought.

In earthquake-prone areas, there is a large body of experience in dealing with seismic-induced liquefaction risk for civil infrastructure and buildings. One of the key elements of that practice (e.g. JGS, 2018) is the resource of ground improvement technologies to modify susceptible soils, so that liquefaction may not occur under design seismic loads. However, it is not always straightforward to translate that experience to TSF flow liquefaction susceptibility remediation.

Ground improvement for seismic liquefaction remediation is most frequently performed in soils with a moderate amount of fines, at depths that rarely exceed 15 m and in level ground conditions. Those characteristics are unlikely to be present at TSF that may benefit from ground improvement.

There is also the issue of intervention risk. In most circumstances where seismic liquefaction remediation is sought in civil infrastructure applications, there is no fear that the ground treatment itself might trigger widespread liquefaction failure, even if some of the most frequently employed remedial technologies, like densification through dynamic compaction, vibro-flotation or vibro-replacement, actually operate by liquefying the ground temporarily around the treatment zone (Han, 2015; Kirsch & Kirsch, 2017). The situation may be very different for a TSF where material susceptible to static liquefaction has been located in a structural zone. Several large-scale TSF failures involving flow liquefaction, like Merriespruit (Fourie et al., 2001; Mánica et al., 2021) or Brumadinho (Arroyo & Gens, 2021) appear to have been triggered by initial failure at a relatively small zone. Any remedial technique predicated on liquefying the ground, even if in a relatively small and contained area, would thus need to consider the risk of uncontained liquefaction propagation destabilizing the structure.

Ground improvement via permeation grouting is one of the gentler liquefaction remedial technologies. In permeation grouting, indeed, a fluid carrying a binder enters the soil voids under low and controlled pressure. The binder sets and cures in the ground, thereby creating a treated soil with larger strength and stiffness and reduced permeability. Permeation grouting is not only one of the oldest technologies in ground improvement, but also one with a fast pace of technological improvement, due to the apparition of new binders (Spagnoli, 2021). Permeation grouting is frequently associated with cohesionless soils (e.g. gravel and sand; Grassi, 2022), but the boundary of applicability of the technique has gradually shifted towards finer materials. For instance, Fraccica et al. (2022) show that binders based on colloidal silica suspensions (CS) are able to successfully permeate soils with as much as 70% silt content.

In seismic liquefaction remediation, CS passive permeation was pioneered by Gallagher et al. (2002; 2007) as a treatment technique well adapted for sites that were difficult to access (e.g. liquefiable soils underlying existing buildings). Passive permeation relies on natural groundwater flow to transport the CS in place before solidification. This is a process that poses some difficulties from the quality assurance viewpoint and large-scale application examples are still scarce. Lately, there has been increased interest in more controlled alternatives, which involve "active" permeation of CS at selected treatment points. Applications in underpinning and tunnel treatments are well documented (Rasouli et al., 2016; Spagnoli et al., 2021). It is then reasonable to ask if these applications may be potentially extended to help remediating liquefiable materials in TSF. The objective of this paper is to obtain some preliminary answers for that question.

The paper is organized in two main sections. Section 2 presents the essential background information, including key aspects of permeation grouting technology and of CS grout rheology as well as the methodological tools necessary for designing a potential treatment. These include some newly developed simplified design formulae that, given some grout and soil characteristics, allow to evaluate the dynamics of key injection features (e.g. applied pressure, extent of treatment). They also include some auxiliary criteria, necessary for overall treatment sizing. Section 3 applies the previous concepts to an idealized, but realistic, case based on the well-known Merriespruit tailing dam (South Africa), which failed by overtopping-induced liquefaction. Different potential CS stabilization treatments are considered, examining their effects on the stability of the dam and evaluating the time required for the treatment.

2 BACKGROUND

2.1 *Fundamentals of permeation grouting*

In most field applications of permeation grouting, injection takes place using the tubes-a-manchette technique (Warner, 2004). An oversized hole is drilled, a PVC pipe with sleeve-ports is inserted and a cement-bentonite grout is used to fill the annular space between pipe and borehole wall. Injection then takes place in sequence from several port holes, spaced at fixed intervals ranging from 0.3 to 0.6 m. A faster and simpler treatment process, however, is possible in soft soils where the steel injection pipe may be just pushed in place. Injection then takes place only through holes located close to the pipe tip, as the pipe is lifted backwards.

The geometry of the treated area at any injection point may be approximated by a sphere, assuming radial grout seepage from each injection source (Han, 2015; Boschi et al., 2022b). Once

the effective radius of injection is estimated, the vertical spacing between injection points (S_z) as well as the spacing in plan (S_x, S_y) between perforations (or treatment points for pushed-in tubes) are specified to define the overall treatment geometry.

Permeation grouting is, as already mentioned, a low-pressure injection technique. If the fluid pressure is raised and the permeation gradients are increased, the mechanics of injection change, and phenomena such as hydraulic fracturing, a.k.a. "claquage", or grout cavity expansion, a.k.a. "compaction" grouting, are expected. This is here avoided by strictly limiting injection pressure p_{inj} (Han, 2015; Boschi et al., 2020; Boschi et al., 2022), so that $p_{inj} < p_{inj,MAX}$. More precisely, the injection usually proceeds with a constant flow rate (Q), whose value is selected so that both $p_{inj} < p_{inj,MAX}$ and a desired radius of injection is attained within a certain injection time t_{inj}.

2.2 *Grouting with colloidal silica suspensions*

Colloidal silica grout of interest in ground permeation takes the form of manufactured aqueous suspensions of nanometric silica particles (SP), solidifying as gel upon addition of salt (typically suspension of sodium chloride, NaCl) at a rate controlled by pH, temperature T, SP and salt concentrations (Bergna & Roberts, 2005). CS grout has several inherent advantages for permeation treatments, such as small particle size, low viscosity and non-toxicity. All these benefits have driven the uptake of CS for ground improvement in geo-environmental (Moridis et al., 1995; Wong et al., 2018) and liquefaction mitigation applications (Gallagher et al., 2007; Zhao et al., 2020).

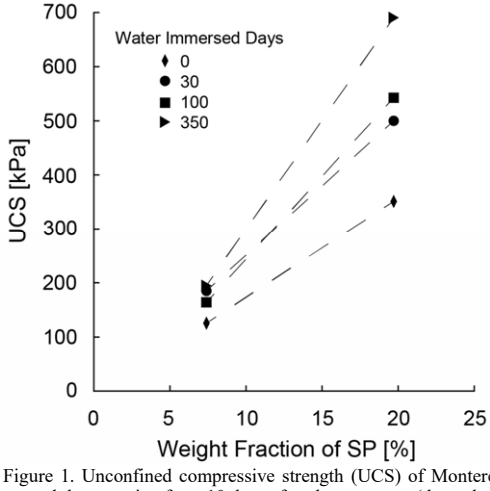

Figure 1. Unconfined compressive strength (UCS) of Monterey sand grouted with CS, under water for several days starting from 10 days after the treatment (data taken from Persoff et al., 1999).

Soils treated with CS become bonded by the silica gel that occupies the pore space. There are numerous experimental campaigns documenting the gain in strength as the SP concentration in the suspension increases (Persoff et al., 1999; Gallagher & Mitchell, 2002; Georgiannou et al., 2017; Spagnoli et al., 2021). For instance, Persoff et al. (1999) observed a linear increase of unconfined compressive strength (UCS) of CS grouted specimens of both Monterey sand and Trevino soil with SP concentration, as well as a continuous increase with time. In Figure 1, UCS results derived by these authors are presented: they refer to sand specimens (i) grouted with CS characterized by SP concentrations of either 7.4% or 19.7% and (ii) immersed in water 10 days after the treatment. The medium- and long-term strength gains of CS treated soils were also documented by Yonekura and Miwa (1993), who tested sand grouted with (presumably undiluted) CS. At 100 days, the strength was 655 kPa and the ultimate strength (registered after 1000 days) was more than twice that value.

The effect of CS on the cyclic properties of the treated soil is also very significant, with large gains in cyclic strength and reductions on pore pressure generation with SP of 10%-15% (Díaz-Rodríguez et al., 2008; Salvatore et al., 2020). Moreover, CS treatments reduce soil hydraulic conductivity significantly with measured values on the treated soil typically below 10^{-8} m/s (Fraccica et al 2022). Therefore, undrained behavior of the threated soil is expected in most circumstances.

Quantifying the complex time-dependent rheological behavior of the CS grouts is crucial for the proper design of permeation treatments. CS grouts have been often described as Newtonian fluids, but Boschi et al. (2022c) firstly observed that a Binghamian description is more realistic for the strain rates commonly encountered in-situ during permeation grouting applications ($\dot{\gamma}$ ranging between 20 and 100 s^{-1}). Moreover, the two key parameters, viscosity (μ) and yield stress (τ_0), increase with time. Once gelling time $t_{gelling}$ is reached, τ_0 increases exponentially and flow is practically stopped.

Several authors, such as Funehag (2012), Agapoulaki & Papadimitriou (2018) and Boschi et al. (2022c), have measured the rheological evolution of CS grouts by means of rheometric tests. The key controlling factors are (i) mix component proportions (i.e. percentages of SP and NaCl and ratio between them), (ii) pH and (iii) T. The interplay of these factors results in a large variety of possible rheologies for CS grouts. The temporal evolutions of Binghamian rheological properties for some CS grouts (Table 1) is reported in Figure 2. Grouts CS1 and CS2 are characteristic of the relatively fast-set grouts that are in demand for tunneling applications, whereas CS3 illustrates a grout with slower gelling, but still much faster than what is typical for passive permeation applications. It can be observed that: (i) $\mu(0)$ is constant and equal to water viscosity (1 mPa·s), (ii) for $t < t_{gelling}$, the μ evolution is significant for the slow-set CS3, contrarily to τ_0 entity, (iii) τ_0 remains constant and increases abruptly after $t_{gelling}$.

Table 1. Characteristics of three different CS grouts.

	Source	*Silica size* [nm]	*SP* [% w]	*NaCl* [% w]	γ [kN/m^3]	*pH* [-]	*T* [°C]
CS1	MasterRoc MP325, MBS Italia (2021)	4	12.7	1.5	11	10.2	20
CS2	MasterRoc MP320, MBS Italia (2021)	16	30	3.75	12	9.5	20
CS3	Agapoulaki & Papadimitriou (2018)	7	10	0.5	11	6	20

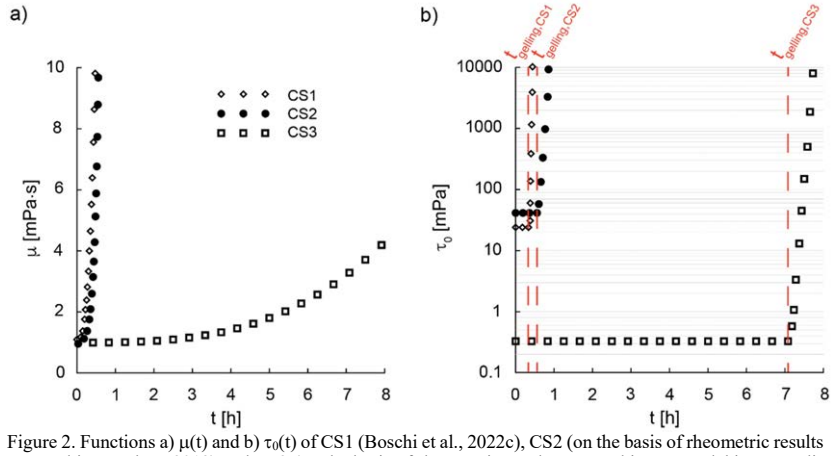

Figure 2. Functions a) $\mu(t)$ and b) $\tau_0(t)$ of CS1 (Boschi et al., 2022c), CS2 (on the basis of rheometric results reported in Funehag, 2012) and CS3 (on the basis of rheometric results reported in Agapoulaki & Papadimitriou, 2018).

2.3 *Design formulae*

Boschi (2022) and Boschi et al. (2022c) have recently presented and validated a modified Darcy's law for the flow of time-dependent Binghamian fluids through porous media. This may be expressed as

$$v(t) = -K(t) \cdot \left\langle 1 - \frac{G(t)}{\gamma} \frac{1}{||\boldsymbol{i}(t)||} \right\rangle \cdot \boldsymbol{i}(t), \tag{1}$$

where $v(t)$ is the seepage velocity, $K(t) = k \cdot \gamma / \mu(t)$ the hydraulic conductivity with k [m^2] the intrinsic permeability, $\boldsymbol{i}(t)$ the hydraulic gradient and $||\boldsymbol{i}(t)||$ its modulus. The Macaulay brackets $\langle \cdot \rangle$ evaluate to zero for negative arguments, returning the argument if positive. Finally, $G(t)$ is a flow correction term affected by rheological term τ_0(t):

$$G(t) = \frac{16}{3} \cdot \frac{\tau_0(t)}{d}, \tag{2}$$

where d is the mean pore throat diameter of the soil. This value may be estimated using granular filter design criteria. For instance, a good proxy for d is diameter d_p of the largest particles that may be transported through the soil porous matrix. This is a function of its coefficient of homogeneity C_u and characteristic diameters D_5 and D_{15} (Figure 3; Kenney et al., 1985).

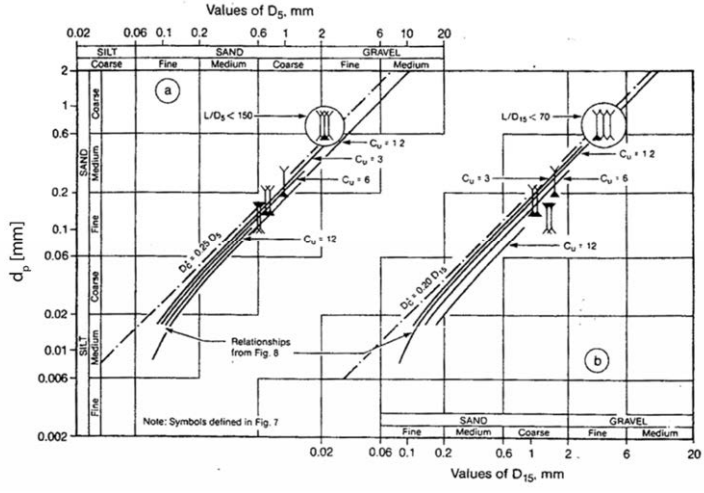

Figure 3. Diameter of the largest particle potentially transported through the soil matrix d_p as a function of soil characteristic diameters (D_5 and D_{15}) and uniformity coefficient C_u (modified figure from Kenney, 1985).

In a further development, Boschi (2022) and Boschi et al. (2022c) used the modified Darcy's law with the time dependent Binghamian fluid rheological properties to obtain closed-form solutions for permeation of grouts in soils starting from either spherical or cylindrical injection sources. In the former case, under reasonable simplifying hypotheses, constant flow rate to be imposed Q^*, radius attained by the injected fluid front r_g and applied injection pressure p_{inj} are observed to be related through the following system of equations:

$$\begin{cases} \langle p_{inj}(t) - G(t) \cdot (r_g(t) - r_0) \rangle - \frac{Q^* \mu(t)}{4\pi k} \cdot \left(\frac{1}{r_0} - \frac{1}{r_g(t)} \right) = 0 \\ r_g(t) - r_0 \cdot \sqrt[3]{1 + \frac{3Q^*}{4\pi n r_0^3} \cdot t} = 0, \end{cases} \tag{3}$$

where the soil parameters include average porosity n, intrinsic permeability k and -through G-

mean pore throat diameter d. The formula also employs radius r_0 of the injection source and the time-dependent rheological parameters of the CS grout employed, $\mu(t)$ and $\tau_0(t)$.
As shown below, these equations may be applied to obtain the whole injection characteristic curves (e.g. the evolution with time of injection both pressure and radius, given an imposed flow rate). They may be also applied to obtain point estimates of the corresponding values for a particular t_{inj}. It is worth noticing that this final or design injection time has to be less than $t_{gelling}$, but not by much, to avoid uncontrolled (passive) grout seepage and remain within the spirit of controlled permeation grouting. As the rheological characteristics of CS grouts remain quite low until $t_{gelling}$, the pressure requirements are limited until the onset of gelling.
Finally, r_0 is established considering a sphere of equal area to the lateral surface of a cylinder given by the zone of the injection tube where the injection ports are located (Boschi et al., 2022b). A reasonable value in case of injections through steel pipes is r_0 = 52 mm.

2.4 *Treatment sizing*

Injection point layout is a key aspect of treatment sizing. Most applications of permeation grouting, for instance in tunneling (AFTES, 1991), are focused on water inflow control and are rather demanding in terms of overlap and improved-ground continuity. On the other hand, cement-based ground improvement for seismic-induced liquefaction remediation is successful with far less denser treatments, involving quadrilateral lattices or unconnected column patterns (JGS, 2018). For a column-based treatment, area ratio AR is the ratio occupied by columns in the treatment unit cell (Han, 2015). Model experiments (Bahmanpour et al., 2019) have shown that column treatment patterns that imply treatment area ratios as low as 35% are reasonably successful to limit the onset of seismic-induced liquefaction. Seismic liquefaction remedial treatments based on cement are typically executed with deep mixing technology, which is more energy intensive than the permeation grouting considered here; however, the observation applies to the final product. Still, as there are no similar studies for the flow liquefaction cases envisaged here, for this feasibility study several triangular patterns of isolated columns were explored, ranging from a very dense pattern of tangent columns (AR = 95%) to less intensive treatments with AR of only 35%.

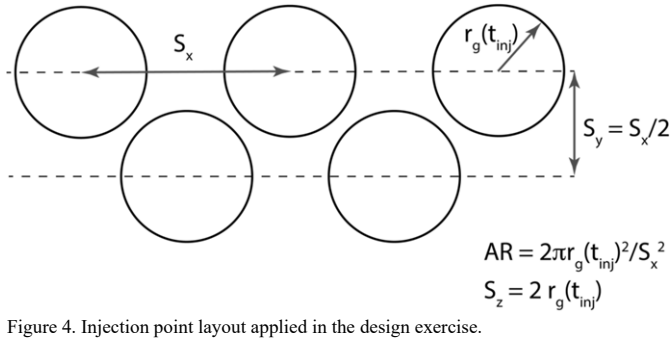

Figure 4. Injection point layout applied in the design exercise.

Figure 4 illustrates the characteristics of the selected triangular column layout in plan view (x-y plane, parallel to the ground surface). As indicated, AR has a direct relation with the basic spacing S_x, whereas $S_y = S_x/2$. Along the vertical direction, conversely, it is assumed that the grout point injections remain in contact so that $S_z = 2\ r_g(t_{inj})$.
Given the overall dimensions of the treatment area (l_x, l_y, l_z), it is then straightforward to find the total number of injection points N_{inj} and compute the overall injection treatment time t_{treat} as follows:

$$t_{treat} = N_{inj} \cdot t_{inj} \,. \tag{4}$$

Apart from strict injection treatment time, some extra time (t_{pipe}) is required to advance and withdraw the injection pipes. This may be computed using the known overall perforation length L_{holes} and assuming that the steel injection pipes move at the standard CPT velocity:

$$t_{pipe} = 2 \cdot \frac{L_{holes}}{0.02\frac{m}{s}}. \quad (5)$$

3 APPLICATION EXAMPLE

3.1 *Case description*

The herein considered case study is based on the Merriespruit tailing dam which failed due to static liquefaction in 1994, a few hours after wall overtopping due to insufficient freeboard and a heavy thunderstorm (Fourie et al., 2001). A stress-deformation analysis of this case by Mánica et al. (2021) has recently confirmed that the conditions of the tailings at Merriespruit were such that a relatively small erosion at the face was sufficient for the initiation and propagation of static liquefaction, leading to a major overall slope failure. Although stress-deformation analyses offer unique insight in the different mechanisms and condition leading to failure, they are somewhat cumbersome and, for comparative parametric analyses, limit equilibrium (LE) is still the tool of choice.

Fourie and Tshabalala (2005) presented several LE analyses of this case using the collapse line approach. In this approach, an effective stress envelope that aims to represent lower bound conditions for the occurrence of static liquefaction is used for design. They found that if the collapse line was parametrized with a friction angle ϕ' = 24.4°, the LE factor of safety (*FoS*) for a dam section such as that depicted in Figure 5 was close to 1. This analysis is taken here as the starting point to evaluate the improvement in stability that may be achieved by means of ground treatment with a CS grout. Three different possible zones for tailing improvement are taken into account (A, B, C), considering first the effect of each treatment on LE *FoS* and then estimating the time required for its execution.

Table 2. Geotechnical parameter values for tailing deposit and foundation.

	γ [kN/m^3]	ϕ' [°]	c' [kPa]	n [-]	K [m/s]	d [mm]
Tailing deposit	20	24.4	0	0.5	10^{-5}	0.008
Foundation	20	40	40	-	-	-

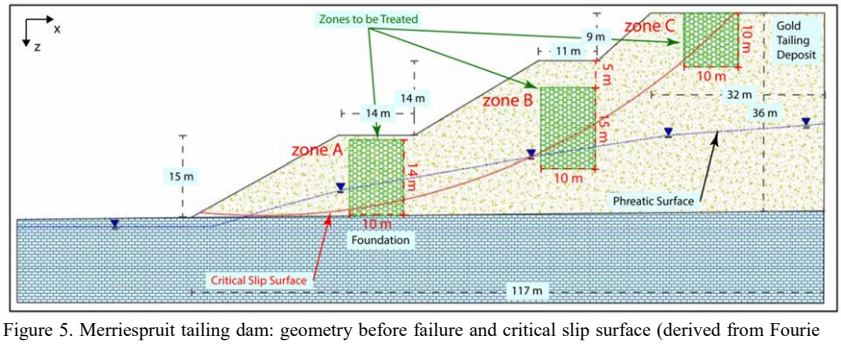

Figure 5. Merriespruit tailing dam: geometry before failure and critical slip surface (derived from Fourie and Tshabalala, 2005), identified zones to be treated (A, B and C).

The geo-mechanical properties for both tailings and foundation, derived from Fourie and Tshabalala (2005) and Torrez Cruz (2016) are summarized in Table 2. Saturated conditions are assumed even above the phreatic surface. The values for n, K and d are representative of tailings

from legacy deposits in Spain (Burbano, 2021); the chosen permeability value would approximately correspond to a 50%-50% sand-silt mixture in the permeation experiments reported by Fraccica et al. (2022).

3.2 *Permeation design*

Once grout rheology and injection flow rate are specified, system of Equations (3) may be employed to derive the evolution of grout front radius and injection pressure until gelling occurs, i.e. for $0 < t < t_{gelling}$. Figure 6 illustrates the corresponding results for (i) CS3 type of grout, (ii) Q = 1, 3 and 5 l/min and (iii) single-point tip injectors (with radius r_0 = 52 mm).
The p_{inj} increase with time (Figure 6a) has two causes: (1) the volume expansion of the injected area, as indicated by the r_g increase in Figure 6b and (2) the evolution of the grout rheological properties. A sharp increase in pressure then indicates the advent of grout gelling. At any given time, larger flow rates result in higher injected radius and injection pressures. Lower flow rates also result in a more gradual pressure raise as gelling approaches, which would be beneficial for control purposes. Note also that if injection at a point is stopped way before gelling takes place, the CS grout will continue flowing, but mostly downwards, because of gravity, and the designed treatment geometry will not be attained.
All these effects need to be considered when selecting injection parameters. For the example application, we have selected a limit injection pressure of $p_{inj,MAX}$ = 2 bar and a flow rate Q^* = 3 l/min. As indicated by the red lines in Figure 6b, this leads to an estimate of $r_g(t_{inj})$ = 83 cm and t_{inj} = 6.7 h, which is about 85% of the estimated $t_{gelling}$.

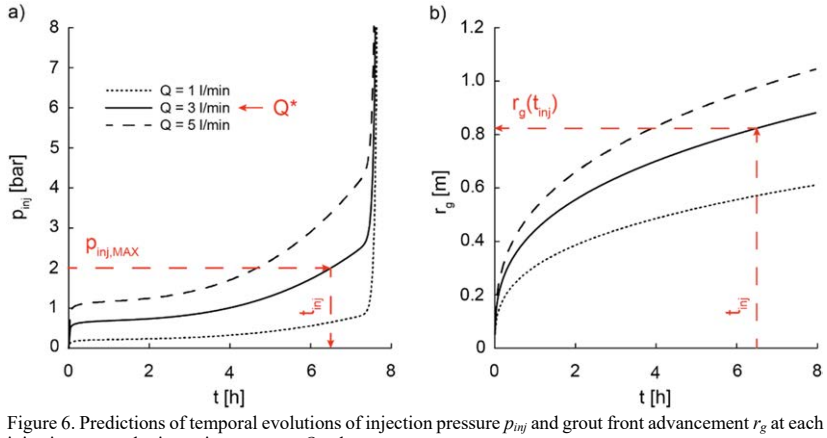

Figure 6. Predictions of temporal evolutions of injection pressure p_{inj} and grout front advancement r_g at each injection source by imposing constant Q values.

3.3 *Effect on slope stability*

Stability is evaluated by LE using the Morgenstern-Price (MG) method as implemented in the Rocscience SLIDE2 software (2021). We only consider deep and circular slip surfaces, to be aligned with those applied in previous LE analyses of the Merriespruit failure, and we use the material parameters of Table 2 for both foundation and untreated tailing deposit.
For the pre-treatment scenario, the slip surface identified by Fourie and Tshabalala (2005; Figure 5) results in a FoS = 1.03, with other similar surfaces being slightly more critical (FoS = 0.99). This is the base case from which ground improvement effectiveness has to be judged.

We consider three possible zones for CS permeation treatment: A, B and C, as illustrated in Figure 5. LE analyses are performed for all 7 different combinations of treatment zones, i.e.: (i) zone A alone, (ii) zone B alone, (iii) zone C alone, (iv) zones A and B, (v) zones A and C, (vi) zones B and C and (vii) all zones A, B and C.

For the areas treated with CS, a fully undrained response is assumed. For a treatment based on CS3 (SP concentration = 10%), we estimate, as a base case, an undrained strength *Su* value equal to 130 kPa ($Su_{treated\_zone}$), according to Figure 1, for conditions 40 days after treatment.

The *FoS* values obtained for different treatment scenarios are presented in Table 3. It turns out that stability improvements are obtained only if either zone A (close to the dam foot) or zone B (in the middle of the dam) are treated. If both of them are treated (case A-B), there is an additional increase in *FoS*. Conversely, in general, there is no significant improvement from treating zone C, either alone or in combination. In Figure 7, the *FoS* analysis conducted in the case of zone C alone is reported and it is evident how, in this case, the slip surface sidesteps the treatment zone.

Increasing strength of the treated zone does increase the *FoS*, as expected. For example, if $Su_{treated\_zone}$ = 200 kPa (Table 3), the *FoS* obtained treating only zone B, for example, is higher than those obtained with two/three treated zones at the lower strength. If zone A is additionally treated, there is a significant safety gain (*FoS* = 1.22). Once again, no remarkable improvements from treating zone C are detected. According to the results in Figure 1, an increased strength for the treated soil may be obtained by increasing SP concentration, considering a longer curing time or both. It was also found that treatments resulting in *Su* values lower than 80 kPa would not stabilize the slope at all, even considering treatment case A-B-C.

Table 3. Safety factor *FoS* for different treatment geometries.

$Su_{treated\_zone}$ [kPa]	CS treatment zones						
	A	B	C	A-B	A-C	B-C	A-B-C
130	1.07	1.11	1	1.15	1.08	1.14	1.16
200	1.14	1.17	1	1.22	1.16	1.17	1.22

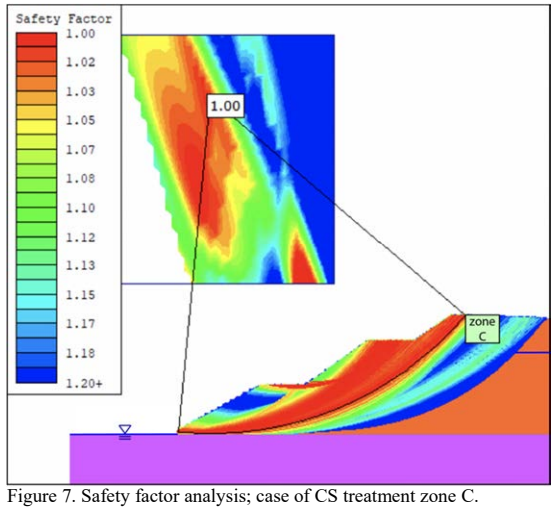

Figure 7. Safety factor analysis; case of CS treatment zone C.

3.4 *Estimation of treatment time*

The overall injection treatment time t_{treat} computed for different treatment scenarios is presented in Table 4. The results are presented in days per m of dam section treatment. The time required to advance and withdraw the pipes t_{pipe} was a fraction (less than 1%) of t_{treat} in all scenarios.

Reducing AR has a very significant effect on treatment time, as expected. Although the times computed per unit m of treatment are significant, it should be noted that the time computation assumes that a single equipment is employed for all the injection work. In practice multiple injectors would be likely to be employed simultaneously for better efficiency.

Table 4. Overall single-team injection treatment time t_{treat} [days/m] for different treatment geometries.

Area ratio	CS treatment zones						
AR	A	B	C	A-B	A-C	B-C	A-B-C
0.95	12	13	9	25	21	22	34
0.70	10	11	8	21	18	19	29
0.50	7	8	5	14	12	13	20
0.35	4	5	3	9	8	8	12

4 CONCLUSIONS

The results obtained suggest that targeted permeation grouting with colloidal silica suspension (CS) grouts may contribute to reduce instability risks in tailing storage facilities (TSF). However, this study is only indicative and would need to be expanded before envisaging field application. To begin with, CS rheology as well as CS treated tailing improvement are strongly dependent on compositional and environmental factors (pH, temperature, presence of salts, etc.), which will be different in different tailings. One-size-fits-all solutions are not possible and local studies will be needed to adapt the CS grout to the material at hand. In this respect, the practices and procedure followed in the design of paste tailings (Yilmaz & Fall, 2017) are a good example of the approach needed. Another aspect that would require further study relates to the effect of different treatment configurations on flow liquefaction. How much treatment (Area ratio) is necessary to impede flow liquefaction propagation throughout a treated zone? What are the safe limits of permeation pressure? Answering these and other questions of mechanical nature would require some well-oriented experimental and numerical research.

The tolerance for risk in TSF operation has sharply decreased in the last decade as a consequence of repeated large-scale failures. When materials that are susceptible to flow liquefaction are identified in structural zones of existing or legacy TSF, remedial options are necessary to de-risk the facility. The work presented here indicates that controlled permeation grouting with colloidal silica grout may be one such option.

5 ACKNOWLEDGEMENTS

We would like to thank MBCC Group for the financial support for the third author and Dr. Davide Grassi for useful discussions on the subject of in-situ applications.

REFERENCES

AFTES (1991). Recommendations on grouting for underground works. Tunnel. Underground Space Technol., 6(4): 383–461.

Agapoulaki, G. I., & Papadimitriou, A. G. (2018). Rheological properties of colloidal silica grout for passive stabilization against liquefaction. Journal of Materials in Civil Engineering, 30(10), 04018251.

Arroyo, M. & Gens, A. (2021) Computational analyses of Dam I failure at the Corrego de Feijao mine in Brumadinho, CIMNE report to VALE (Researchgate https://tinyurl.com/4zu8ymeh).

Bahmanpour, A., Towhata, I., Sakr, M., Mahmoud, M., Yamamoto, Y., & Yamada, S. (2019). The effect of underground columns on the mitigation of liquefaction in shaking table model experiments. Soil Dynamics and Earthquake Engineering, 116, 15-30.

Bergna, H. E., & Roberts, W. O. (2005). Colloidal silica: fundamentals and applications. CRC Press.

Boschi, K., di Prisco, C. G., & Ciantia, M. O. (2020). Micromechanical investigation of grouting in soils. International Journal of Solids and Structures, 187, 121-132.

Boschi, K. (2022). Permeation grouting in granular materials. From micro to macro, from experimental to numerical and viceversa. PhD Thesis. Politecnico di Milano. http://hdl.handle.net/10589/182992

Boschi, K., Ciantia, M. O., & Di Prisco, C. G. (2022, May). Pressure grouting of microfine cements in soils: micromechanical processes. In 20th International Conference on Soil Mechanics and Geotechnical Engineering (pp. 621-626). Australian Geomechanics Society.
Boschi, K., Grassi, D., Castellanza, R., & di Prisco, C. (under review – 2022b) Permeation Grouting in Soils: Numerical Investigation and Modelling. Proceedings of the Institution of Civil Engineers – Ground Improvement.
Boschi, K., di Prisco, C., Grassi, D., Modoni, G. & Salvatore, E. (under review – 2022c). Nanosilica Grout Permeation in Sand: Experimental Investigation and Modelling. Géotechnique.
Burbano, D. A. (2021). Ground improvement for tailing dam remediation and design MSc thesis. UPC. Retrieved from http://hdl.handle.net/2117/35994
Díaz-Rodríguez, J. A., Antonio-Izarraras, V. M., Bandini, P., & López-Molina, J. A. (2008). Cyclic strength of a natural liquefiable sand stabilized with colloidal silica grout. Canadian Geotechnical Journal, 45(10), 1345-1355.
Fourie, A. B., Blight, G. E., & Papageorgiou, G. (2001). Static liquefaction as a possible explanation for the Merriespruit tailings dam failure. Canadian Geotechnical Journal., pp. 707-719. doi:10.1139/cgj-38-4-707
Fourie, A. B., & Tshabalala, L. (2005). Initiation of static liquefaction and the role of K0 consolidation. Canadian Geotechnical Journal, pp. 892-906.
Fraccica, A., Spagnoli, G., Romero, E., Arroyo, M., & Gómez, R. (2022). Permeation grouting of silt-sand mixtures. Transportation Geotechnics, 35, 100800.
Funehag, J. (2012). Guide to grouting with silica sol - for sealing in hard rock. Stockholm: Stiftelsen Bergteknisk Forskning Rock Engineering Research Foundation.
Gallagher, P. M., & Mitchell, J. K. (2002). Influence of colloidal silica grout on liquefaction potential and cyclic undrained behavior of loose sand. Soil Dynamics and Earthquake Engineering, 22(9-12), 1017-1026.
Gallagher, P. M., Conlee, C. T., & Rollins, K. M. (2007). Full-scale field testing of colloidal silica grouting for mitigation of liquefaction risk. Journal of Geotechnical and Geoenvironmental Engineering, 133(2), 186-196.
Georgiannou, V. N., Pavlopoulou, E. M., & Bikos, Z. (2017). Mechanical behaviour of sand stabilised with colloidal silica. Geotechnical Research, 4(1), 1-11.
Grassi, D. (2022). Tecnologie innovative per il consolidamento di substrati di fondazione e opere geotecniche. PhD Thesis. Bicocca University. https://boa.unimib.it/handle/10281/366246
Han, J. (2015). Principles and Practices of Ground Improvement. New Jersey: Wiley & Sons.
Iler, K. R. (1979). The chemistry of silica. Solubility, polymerization, colloid and surface properties and biochemistry of silica.
ICMM, (2021). Tailings management: good practice guide, International Council for Mining and Metals. https://www.icmm.com/website/publications/pdfs/environmental-stewardship/2021/guidance_tailings-management.pdf
JGS (Japanese Geotechnical Society) (2018). Remedial Measures Against Soil Liquefaction: from Investigation and Design to Implementation. Routledge.
Kenney, T. C., Chahal, R., Chiu, E., Ofoegbu, G. I., Omange, G. N., & Ume, C. A. (1985). Controlling constriction sizes of granular filters. Canadian Geotechnical Journal, 22(1), 32-43.
Kirsch, K., & Kirsch, F. (2017). Ground improvement by deep vibratory methods (p. 252). Taylor & Francis.
Liao, H. J., Huang, C. C., & Chao, B. S. (2003). Liquefaction resistance of a colloid silica grouted sand. In Grouting and ground treatment (pp. 1305-1313).
Mánica, M, Arroyo, M, Gens, A & Monforte, L. (2021) Application of a critical state model to the Merriespruit tailings dam failure, accepted for publication in ICE Journal of Geotechnical Engineering.
MBS Italia (2021). Technical datasheets of MasterRoc products. https://www.master-builders-solutions.com/it-it/products/masterroc
Moridis, G. J., Persoff, P. G., Apps, J. A., Myer, L., & Pruess, K. (1995). A Field Test of Permeation Grouting in Heterogenous Soils Using a New Generation of Barrier Liquids.
Persoff, P., Apps, J., Moridis, G., & Whang, J. M. (1999). Effect of dilution and contaminants on sand grouted with colloidal silica. Journal of geotechnical and geoenvironmental engineering, 125(6), 461-469.

Rasouli, R., Hayashi, K., & Zen, K. (2016). Controlled permeation grouting method for mitigation of liquefaction. Journal of Geotechnical and Geoenvironmental Engineering, 142(11), 04016052.

Rocscience Inc. 2021, Slide2, computer software, https://www.rocscience.com/software/slide2

Salvatore, E., Modoni, G., Mascolo, M. C., Grassi, D., & Spagnoli, G. (2020). Experimental Evidence of the Effectiveness and Applicability of Colloidal Nanosilica Grouting for Liquefaction Mitigation. Journal of Geotechnical and Geoenvironmental Engineering, 146(10), 04020108.

Spagnoli, G. (2021). A review of soil improvement with non-conventional grouts. In-ternational Journal of Geotechnical Engineering, 15, 3, 273-287. https://doi.org/10.1080/19386362.2018.1484603

Spagnoli, G., Seidl, W., Romero, E., Arroyo, M., Gómez, R., & López, J. (2021). Unconfined compressive strength of sand-fines mixtures treated with chemical grouts. In Geotechnical Aspects of Underground Construction in Soft Ground (pp. 829-835). CRC Press.

Torres Cruz, L. A. (2016). Use of the cone penetration test to assess the liquefaction potential of tailings storage facilitiesq. Johannesburg.

Warner, J. (2004). Practical handbook of grouting: soil, rock, and structures. John Wiley & Sons.

Wong, C., Pedrotti, M., El Mountassir, G., & Lunn, R. J. (2018). A study on the mechanical interaction between soil and colloidal silica gel for ground improvement. Engineering geology, 243, 84-100.

Yilmaz, E., & Fall, M. (2017). Introduction to paste tailings management. In Paste Tailings Management (pp. 1-5). Springer, Cham.

Yonekura R., and Miwa, M. (1993). ‘‘Fundamental properties of sodium silicate based grout.’’ Proc., 11th South East Asian Geotechnical Con- ference, Singapore.

Zhao, M., Liu, G., Zhang, C., Guo, W., & Luo, Q. (2019). State-of-the-art of colloidal silica-based soil liquefaction mitigation: An emerging technique for ground improvement. Applied Sciences, 10(1), 15.